



Preparation of the stimuli-responsive ZnS/PNIPAM hollow spheres

Huei-Kuan Fu^a, Shiao-Wei Kuo^{b,**}, Chih-Feng Huang^a, Feng-Chih Chang^{a,*}, Han-Ching Lin^a

^a Institute of Applied Chemistry, National Chiao-Tung University, Science Building 2, Hsin-Chu, Taiwan

^b Department of Materials and Optoelectronic Science, Center for Nanoscience and Nanotechnology, National Sun Yat-Sen University, Kaohsiung, Taiwan

ARTICLE INFO

Article history:

Received 20 November 2008

Received in revised form

29 December 2008

Accepted 9 January 2009

Available online 14 January 2009

Keywords:

Hollow sphere

Micelle

Quantum dot

ABSTRACT

Novel quantum dots ZnS/poly(*N*-isopropylacrylamide) (PNIPAM) hybrid hollow spheres were obtained by localizing free radical polymerization of NIPAM and crosslinker (MBA) at the peripheral of PCL nanoparticles, followed by biodegradation of PCL with an enzyme of the Lipase PS. The formation of ZnS/PNIPAM hollow spherical structures and the thermo-sensitive reversible properties was systematically investigated by transmission electron microscopy (TEM) and dynamic light scattering (DLS), respectively. The ZnS/PNIPAM hollow spheres possess the photoluminescence properties and a swelling and de-swelling at about 32 °C, which agrees well with the slight red shift in photoluminescence spectra.

© 2009 Elsevier Ltd. All rights reserved.

1. Introduction

Novel materials based on colloidal semiconductor nanocrystals (quantum dots, QDs) have attracted considerable attention in recent years for their special electronic and optical properties coming from quantum confinement effect [1–12]. Most synthetic procedures involved for colloids or capped free-standing powders yield crystallites with a relatively larger size distribution. As a result, a capping agent such as mercaptoethanol has been used to covalently bond on the surface atoms of the nanocrystallites, making them stable under normal atmospheric condition [13,14]. Zinc sulfide (ZnS), a II–VI group semiconductor, is particularly suitable for use as host material for large variety of dopants because of its 3.7 eV band gap [15], and is widely used in flat panel displays, infrared windows, sensors, etc. Nanostructured doped ZnS materials have many applications because of their superior luminescence characteristics compared to their bulk counterparts [16–18]. Embedding QDs nanocrystals into polymer matrices is an effective method of enhancing the optical properties of these materials [19]. Zhang [20,21] and Bai et al. [22] have reported the syntheses of polymer composites containing QDs from different polymer matrices.

In addition, stimuli-responsive polymers have attracted great interest for their physical or chemical changes in response to external changes in environmental conditions such as temperature,

pH, ionic strength, and electromagnetic radiation [23]. Poly (*N*-isopropyl acrylamide) (PNIPAM) is a well-known example which undergoes a sharp coil–globule transition in water at 32 °C, changing from a hydrophilic state below this temperature and a hydrophobic state above it [24]. Temperature at the lower critical solution temperature (LCST) corresponds to the region in the phase diagram where the enthalpic contribution of water hydrogen-bonded to the polymer chain becomes less than the entropic gain of the system as a whole and thus is largely dependent on the hydrogen-bonding capabilities of the constituent monomer units.

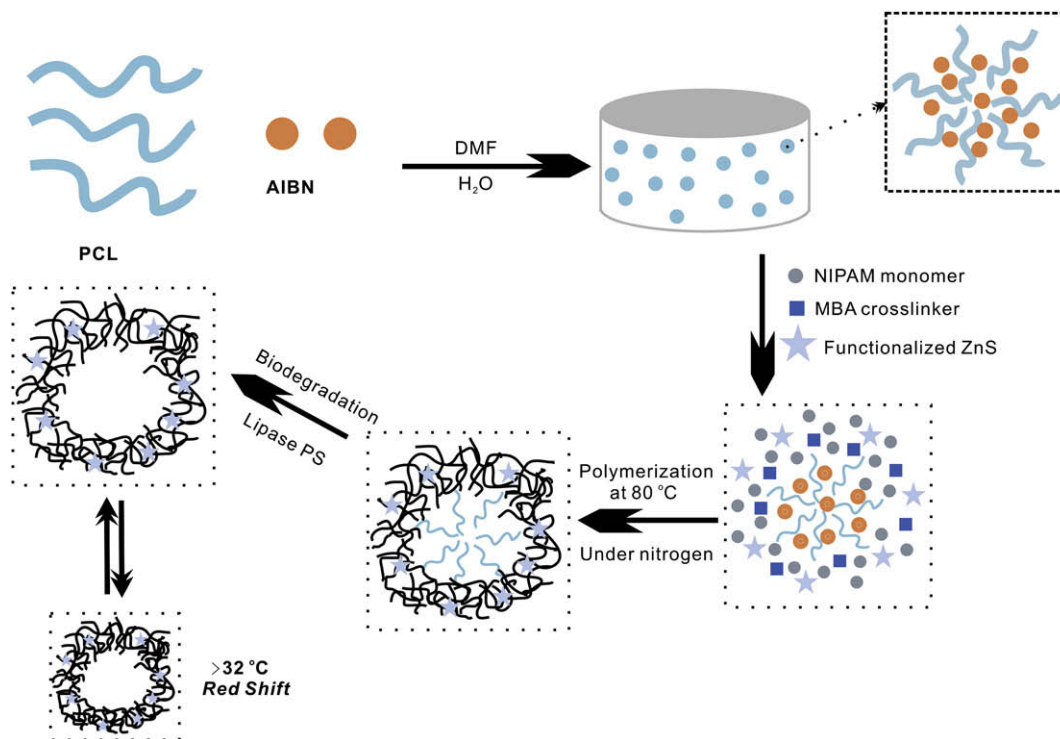
Furthermore, biocompatible, biodegradable and non-toxic synthetic aliphatic polyesters, such as poly(ϵ -caprolactone) (PCL), are very useful in biomedical applications, especially as drug delivery devices [25], because they are completely biodegradable inside the body after its interaction with body fluid, enzyme and cells. Lipase pseudomonas is able to accelerate the biodegradation of PCL, and completed after 6 h in a buffer solution containing the enzyme. Jiang et al. [26] reported that the PCL/PNIPAM core–shell particles were obtained by localizing the polymerization around the PCL nanoparticles then followed by degrading the PCL core with enzyme. The hollow spheres are thermo-sensitive and display a reversible swelling and de-swelling behavior at 32 °C.

In our previous study [27], we reported a simple route to hierarchical ZnS nanoparticle/polymer nanofiber structures through self-assembly of zinc dimethacrylate (Zn(MA)2) in water/ethanol solution by combined use of γ -irradiation polymerization and gas/solid reaction. In this study, we would like to combine the ZnS QDs with PCL/PNIPAM core–shell particles through the AIBN initiated free radical polymerization and then followed by biodegradation of the PCL cores using a commercial enzyme to form hollow spheres.

* Corresponding author. Tel./fax: +886 3 5131512.

** Corresponding author. Fax: +886 7 5254099.

E-mail addresses: kuosw@faculty.nsysu.edu.tw (S.-W. Kuo), changfc@mail.nctu.edu.tw (F.-C. Chang).



Scheme 1. Representation of the photoluminescence hollow sphere preparation and temperature responsive.

The photoluminescence properties of the ZnS/PNIPAM hollow spherical materials of the thermal sensitive polymer can be mediated by temperature changes.

2. Experimental

2.1. Materials

N-isopropylacrylamide (NIPAM) and methacryloyl chloride (stabilized with MEHQ) were obtained from the Tokyo Chemical Industrial CO., Ltd. *N*-isopropylacrylamide monomer (NIPAm) was recrystallized from hexanes and dried in vacuum prior to use. Most chemicals used in this study, including 2-mercaptoethanol, amino Lipase PS from *Pseudomonas cepacia*, phosphate buffer solution 0.1 M, *N,N'*-Methylenebis(acrylamide) (MBA), sodium sulfide non-hydrate (Na₂S·9H₂O) were acquired from the Aldrich Chemical Co., Inc. 4-Dimethylaminopyridine (DMAP), and zinc acetate dehydrate (C₄H₆O₄Zn·2H₂O) were obtained from Acros Organics, USA. 2,2'-Azobis-isobutyronitrile (AIBN), and NaHCO₃ were purchased from Showa, Tokyo. *N,N*-Dimethylformamide (DMF), tetrahydrofuran (THF), and methanol were purchased from the TEDIA Company. The THF was distilled from finely ground CaH₂ before use.

2.2. Preparation of the prepolymers of poly(ϵ -caprolactone)

Tempo-OH (0.0728 g, 2.5×10^{-4} mol) in toluene (5 mL) and 0.2 mL of a toluene solution of triethylaluminum (0.1 mol/L) were mixed under an argon atmosphere. The reaction mixture was stirred at room temperature for 30 min and then allowed to evaporate to remove the byproduct 2-propanol. After repeating this procedure several times, 25 mL dry toluene and 5 mL caprolactone (0.044 mol) were added to the reaction mixture in ice bath. The polymerization was carried out at 25 °C for 24 h under argon and was terminated by adding excess acetic acid (0.2 mL acetic acid/

0.8 mL toluene). Two-thirds of the initial solvent was evaporated, and the residue was precipitated into methanol. The product was dried to constant weight under vacuum.

2.3. Synthesis of the capping agent 2-mercaptoethyl methacrylate

The capping agent was synthesized through the reaction of 2-mercaptoethanol and methacryloyl chloride using DMAP as catalyst. The solution of 2-mercaptoethanol (0.1 mol), methacryloyl chloride (0.12 mol), and DMAP (0.12 mol) in tetrahydrofuran (300 mL) was stirred at room temperature until the reaction was completed. The solid by-products were removed by filtration. The

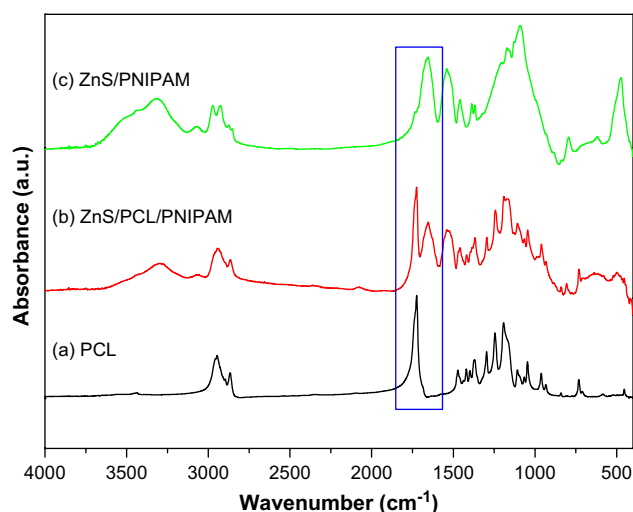


Fig. 1. FT-IR spectra of the (a) PCL, (b) ZnS/PCL/PNIPAM spheres, and (c) ZnS/PNIPAM hollow spheres.

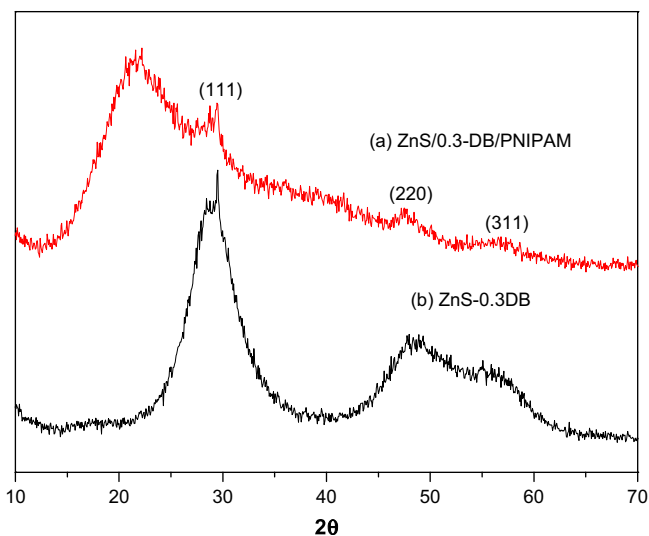


Fig. 2. X-ray diffraction patterns of the (a) ZnS nanoparticle and (b) ZnS/PNIPAM hollow spheres.

solvent was removed in a rotary evaporator at room temperature and the resulted crude product was purified by dissolving in ether and washed several times with NaHCO_3 solution and distilled water. The purified product in ether solvent was dried with anhydrous sodium sulfate, followed by evaporation of the ether under vacuum to afford the 2-mercaptoethyl methacrylate. ^1H NMR (CDCl_3 , $\delta = \text{ppm}$): 6.09, 5.56, 1.96 ($-\text{CH}_2=\text{CH}-$), 4.23, 3.21 ($-\text{O}-\text{CH}_2-\text{CH}_2-$), 1.1 ($-\text{SH}$). FT-IR: 1668 cm^{-1} for $\text{C}=\text{C}$ group, and the 1721 cm^{-1} for $\text{C}=\text{O}$ group.

2.4. Preparation of ZnS nanoparticle peripherally with methacrylate

The thio-capped ZnS nanoparticles were prepared through the reaction of zinc acetate dihydrate (0.01 mol) and 2-mercaptoethyl methacrylate (0.003 mol) in 150 mL of methanol. Na_2S dissolved in a mixture of 40 mL of water and 40 mL of methanol was added and the resulting suspension was stirred for 1 day under nitrogen. The white precipitate was separated by centrifugation (15,000 rpm, 20 min) and the powder sample was dried under vacuum at room temperature.

2.5. Synthesis of QDs hollow spheres

The initiator (AIBN, 0.011 g) and PCL ($M_w \sim 37890\text{ g/mol}$, 0.1 g) were dissolved in DMF (10 mL) and then the solution was added dropwise into deionized water (80 mL). The solution was stirred continually for 1 h then the NIPAM monomer (0.5 g), ZnS nanoparticle (0.1 g) and MBA crosslinker (0.068 g) were added into the suspension solution. The reaction was carried out for 4 h at 80°C under nitrogen. The ZnS/PNIPAM hollow spheres were prepared by using lipase PS to degrade PCL core. The Lipase PS was purified by dissolving it in a 0.1 M phosphate buffer solution. The solution was stirred at 50°C for 6 h and then the hollow spheres were separated by centrifugation (15000 rpm, 10 min), washed by deionized water for several times (Scheme 1).

3. Characterizations

Wide-angle X-Ray diffraction (WAXD) spectrum was recorded on powdered sample using a Rigaku D/max-2500 type X-ray diffraction instrument. The radiation source used was Ni-filtered, $\text{Cu K}\alpha$ radiation ($\lambda = 1.54\text{ \AA}$). The sample was mounted on a circular sample holder, the scanning rate was $0.6^\circ/\text{min}$ from $2\theta = 3$ to 20. Transmission electron microscopy (TEM) images were obtained using a Hitachi H-7500 instrument with an accelerating voltage of 100 kV. The TEM samples were deposited from the ZnS/PNIPAM hollow spheres onto the carbon-coated copper grids. Molecular weights and molecular weight distributions were determined by gel permeation chromatography (GPC) using a Waters 510 HPLC equipped with a 410 Differential Refractometer, a refractive index (UV) detector, and three Ultrastayragel columns (100, 500, and 10^3 \AA) connected in series in order of increasing pore size. The molecular weight calibration curve was obtained using polystyrene standards. ^1H NMR spectroscopic analyses were performed using a Varian Uniytinova-500 NMR Spectrometers at 500 MHz. All spectra were recorded using CDCl_3 as the solvent and TMS as the external standard. Fourier transformation infrared (FT-IR) spectra were recorded at 25°C using a Nicolet AVATAR 320 FT-IR spectrometer; the sample was cast onto KBr pellets from CHCl_3 solution. All FT-IR spectra were obtained within the range $4000\text{--}400\text{ cm}^{-1}$; 32 scans were collected at a resolution of 1 cm^{-1} while samples were purged with nitrogen to ensure that the films remained. Dynamic Light Scattering (DLS) measurements were performed on a Brookhaven 90 plus model

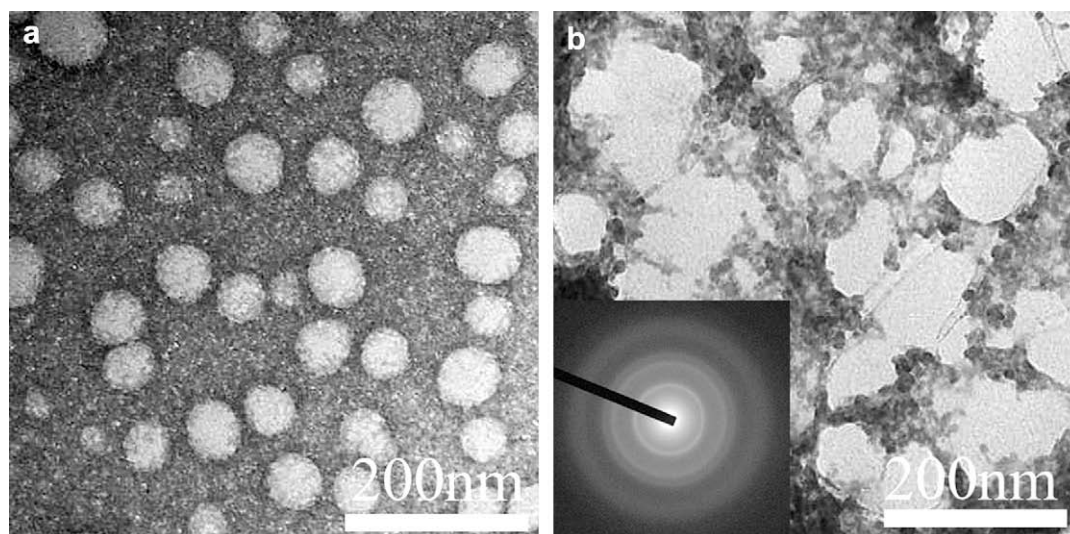


Fig. 3. TEM image and electron diffraction pattern of the (a) PNIPAM hollow spheres and (b) ZnS/PNIPAM hollow spheres.

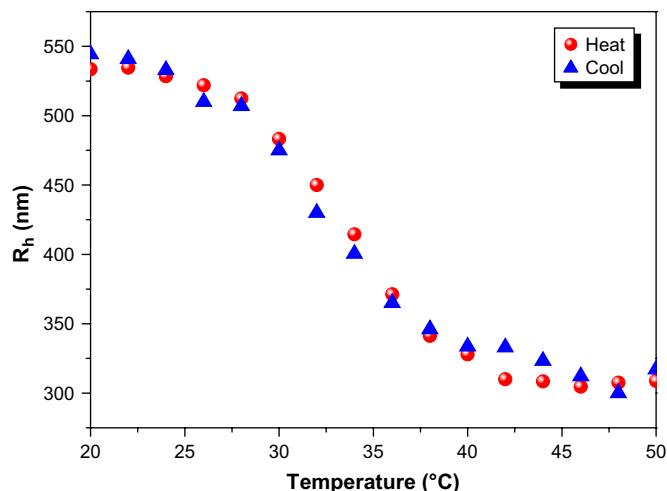


Fig. 4. Variation of average hydrodynamic diameters (D_h) vs. temperature of the ZnS/PNIPAM hollow spheres.

equipment (Brookhaven Instruments Corporation, USA) with a He-Ne laser with a power of 35 mW at 632.8 nm. The temperature was controlled by heating and cooling process, and the measurements were done at an angle of 90° . Photoluminescence (PL) excitation and emission spectra were collected at room temperature using a monochromatized Xe light source.

4. Results and discussion

Fig. 1(a) shows infrared spectroscopy of pure PCL prepared by TEMPO polymerization, where the absorption peaks of carbonyl group of pure PCL are at 1724 cm^{-1} and 1734 cm^{-1} corresponding to crystalline and amorphous phases, respectively. A new absorption of the ZnS/PCL/PNIPAM at 1655 cm^{-1} is attributed to the carbonyl amide group of PNIPAM, indicating the formation of PCL/PNIPAM core-shell spheres. The enzyme of Lipase PS is known to be the degradation enzyme for PCL [28], and it was used as the biocatalyst to degrade the PCL cores in this study. Apparently, the absorption peak of the carbonyl group at 1724 cm^{-1} of PCL was totally disappeared, indicating that the PCL cores were biodegraded completely by using the enzyme of Lipase PS while the absorption

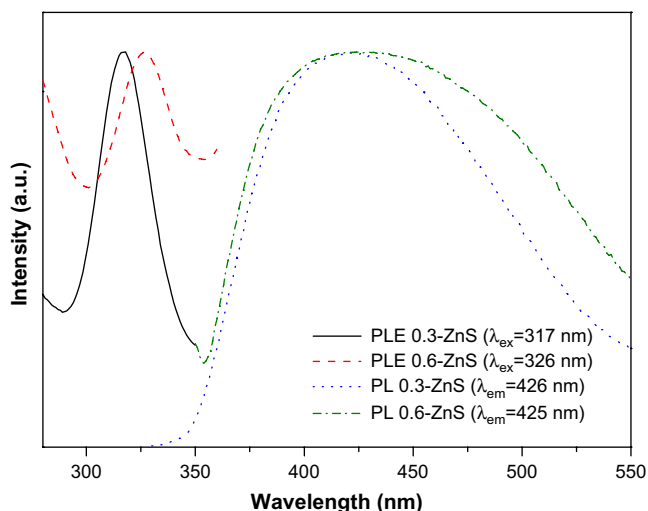


Fig. 5. PLE and PL spectrum of the 0.3-ZnS and 0.6-ZnS nanoparticles.

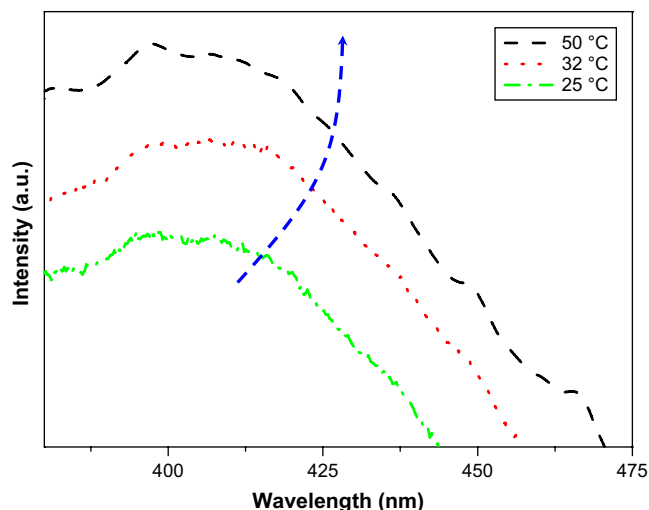


Fig. 6. Normalized photoluminescence spectra of the 0.3-ZnS/PNIPAM hollow sphere at different temperature.

at 1655 cm^{-1} of PNIPAM was still remained as shown in Fig. 1(c), showing the formation of the hollow spheres with QDs.

Fig. 2 shows X-ray diffraction patterns of the ZnS nanocrystallites (a) and ZnS/PNIPAM hollow spheres (b). The three broadened peak positions appeared at 2θ value 29.5° , 48.9° , and 55.1° correspond to the (110), (220), and (311) planes of the cubic crystalline ZnS as shown in Fig. 2(a). An average crystallite size was estimated as ca. 2.7 nm, according to the line width analysis of the (110) diffraction peak based on Debye–Scherrer formula [29], given by $L = (0.9\lambda)/(B\cos\theta)$. L is the coherence length related to particle diameter $D = 3/4L$, B is the full width at the half maximum (FWHM) of the peak (110), λ is the wavelength of the X-ray radiation, and θ is the angle of diffraction. In addition, the ZnS/PNIPAM hollow spheres show the similar diffraction pattern as the pure ZnS nanocrystallites except showing strong PNIPAM amorphous halo around 20° , indicating the successful introducing the ZnS QDs within the PNIPAM hollow sphere matrix.

Fig. 3 shows TEM images of the PNIPAM and ZnS/PNIPAM hollow spheres. In Fig. 3(a), the image of PNIPAM hollow spheres shows no internal structure, indicating the degradation of PCL core, which is consistent with previous study by Jiang et al. [26]. The TEM image of the ZnS/PNIPAM hollow spheres in Fig. 3(b) reveals that dense ZnS nanoparticles having diameters of ca. 3–4 nm are well dispersed within the PNIPAM hollow shells. The selective-area electron diffraction (SAED) pattern (inset to Fig. 3(b)) corresponds to the (111), (220), and (311) planes of crystalline ZnS, indicating that these ZnS nanoparticles in the PNIPAM hollow shells possessing zinc blende crystal structure as the results of X-ray diffraction patterns [Fig. 2].

Dynamic light scattering (DLS) was employed to determine the hydrodynamic diameters ($\langle D_h \rangle$) of the ZnS/PNIPAM hollow spheres and their temperature-responsive swelling and de-swelling behavior. As shown in Fig. 4, as the temperature increased from 20 to 50°C , the average hydrodynamic diameter of the ZnS/PNIPAM hollow spheres decreased from 544 to 317 nm, corresponding to the “swelling” and “de-swelling” states of the crosslinked PNIPAM shell, respectively. These ZnS/PNIPAM hollow spheres clearly display dimensional change with temperature, implying that volumes of these PNIPAM hollow shells can shrink or swell with temperature changes. Most importantly, the reversibility of the size dependence of the hollow shells in the heating process coincides with that in the cooling process. Furthermore, after a cycle of the temperature increase and decrease, the hollow sphere size returns to its starting value.

In addition, PLE results indicate that excitation spectrum of the 0.3-ZnS and 0.6-ZnS nanoparticles are 317 and 326 nm. The number of the 0.3 indicates the mole ratio of the ZnS and capping agent. Fig. 5 showing a slight red shift compared with higher capping agent content. The emission peak for the 0.3-ZnS and 0.6-ZnS are 426 and 425 nm, respectively. PL maximum peak was slightly blue shifted (about 14 nm) relative to that of bulk ZnS (440 nm) and thus exhibiting quantum size effect [30,31].

Poly(*N*-isopropylacrylamide) (PNIPAM) is a well-known thermoresponsive polymer exhibiting a coil-globule transition in aqueous at a lower critical solution temperature (LCST) of around 32 °C [32,33]. Yubai et al. reported that photoluminescence intensities of the PNIPAM/CdTe gels decrease with the increase of temperature [22]. It can be seen the PL intensities of the hollow spheres decreases with the increase of temperature. In the polymer phase transition regime, hydrogen bonds between side groups and water molecules are broken, and PNIPAM undergoes changes in conformation on increasing temperature. At higher temperature above LCST, the PL intensity of 0.3-ZnS/PNIPAM hollow spheres is lower because of the QDs in the PNIPAM hollow spheres shrink due to the increase of hydrophobicity at temperatures above LCST. As a result, these ZnS nanoparticles become closer and closer or even contact each others. Below the LCST, the PL intensity of ZnS/PNIPAM hollow spheres is higher, indicating that these ZnS QDs are well dispersed and separated in the PNIPAM matrix. From the PL results, the peak position of the ZnS/PNIPAM hollow spheres shows slight red shift with the increase of temperature, as shown in Fig. 6. Similar results have been reported that the PL peaks of the CdTe nanocrystals shift to longer wavelengths with larger particles [34].

5. Conclusions

The novel inorganic/organic nano-spheres, (ZnS/PCL/PNIPAM), were successfully prepared by a simple free radical polymerization method. After locking the sphere structure by the cross-linking with the MBA, the core was degraded with Lipase PS, and the ZnS/PNIPAM hollow spheres can be obtained. The ZnS/PNIPAM hollow sphere possesses reversible thermo-sensitive properties and its hydrodynamic diameter (D_h) is sensitive to the temperature stimuli response. Furthermore, slight red shift of maximum PL wavelengths was observed. The hollow spheres of the ZnS/PNIPAM have the potential applications in QDs-based biosensors and devices.

Acknowledgments

The authors thank the National Science Council, Taiwan, for financially supporting this research under Contract NSC-96-2120-M-009-009.

References

- [1] Tagaya A, Ohkita H, Mukoh M, Sakaguchi R, Koike Y. *Science* 2003;301:812.
- [2] Kasai H, Nalwa HS, Oikawa H, Okada S, Matsuda H, Minami N, et al. *Jpn J Appl Phys Part 1* 1992;31:L1132.
- [3] Fujita S, Kasai H, Okada S, Oikawa H, Fukuda T, Matsuda H, et al. *Jpn J Appl Phys Part 1* 1999;38:L659.
- [4] Okada S, Matsuda H, Nakanishi H, Kato M, Muramatsu S. *Jpn Patent Application* 61-192 404; 1982.
- [5] Okada S, Matsuda H, Nakanishi H, Kato M, Muramatsu R. *Jpn Patent* 716 929; 1992.
- [6] Nakanishi H, Matsuda H, Okada S, Kato M. *Mater Res Soc Int Mtg Adv Mater* 1989;1:97.
- [7] Marder SR, Perry JW, Schaefer WP. *Science* 1989;245:626.
- [8] Bhargava RN, Gallagher D, Hong X, Nurmikko A. *Phys Rev Lett* 1994;72:416.
- [9] Schmidt T, Muller G, Spanhel L, Kerkel K, Forchel A. *Chem Mater* 1998;10:65.
- [10] Sapra S, Prakash A, Ghangrekar A, Periasamy N, Sarma DD. *J Phys Chem B* 2005;109:1663.
- [11] Chen W, Malm JO, Zwiller V, Wallenberg R, Bovin JO. *J Appl Phys* 2001; 89:2671.
- [12] Hines MA, Sionnest PG. *J Phys Chem* 1996;100:468.
- [13] Huang F, Zhang H, Banfield JF. *J Phys Chem B* 2003;107:10470.
- [14] Vogel W, Borse PH, Deshmukh N, Kulkarni SK. *Langmuir* 2000;16:2032.
- [15] Ding JX, Zapfen JA, Chen WW, Lifshitz Y, Lee ST, Meng XM. *Appl Phys Lett* 2004;85:2361.
- [16] Sooklal K, Cullum BS, Angel SM, Murphy CJ. *J Phys Chem* 1996;100:4551.
- [17] Suyver JF, Wuister SF, Kelly JJ, Meijerink A. *Nano Lett* 2001;1:429.
- [18] Dinsmore AD, Hsu DS, Gray HF, Qadri SB, Tian Y, Ratna BR. *Appl Phys Lett* 1999;75:802.
- [19] Xu S, Zhang J, Paquet C, Lin Y, Kumacheva E. *Adv Funct Mater* 2003;13:468.
- [20] Ye J, Hou Y, Gui Z, Zhang G. *Langmuir* 2008;24:2727.
- [21] Hou Y, Ye J, Gui Z, Zhang G. *Langmuir* 2008;24:9682.
- [22] Li J, Hong X, Liu Y, Li D, Wang Y, Li J, et al. *Adv Mater* 2005;17:163.
- [23] Gil ES, Hudson SM. *Prog Polym Sci* 2004;29:1173.
- [24] Schild HG. *Prog Polym Sci* 1992;17:163.
- [25] Wang Y, Tang L, Sun T, Li C, Xiong M, Wang J. *Biomacromolecules* 2008;9:388.
- [26] Zhang Y, Jiang M, Zhao J, Ren X, Chen D, Zhang G. *Adv Funct Mater* 2005; 15:695.
- [27] Kuo SW, Chang FC. *J Phys Chem C* 2008;112:16470.
- [28] Nie T, Zhao Y, Xie Z, Wu C. *Macromolecules* 2003;36:8825.
- [29] Guinier A. *X-ray diffraction*. San Francisco, CA: Free Man; 1963.
- [30] Yin XJ, Yan J, Zhi LZ, Xu SH. *J Cryst Growth* 1998;191:692.
- [31] Ghosh G, Naskar MK, Patra A, Chatterjee M. *Opt Mater* 2006;26:1047.
- [32] Otake K, Inomata H, Konno M, Saito S. *Macromolecules* 1990;23:283.
- [33] Kubota K, Fujishige S, Ando I. *J Phys Chem* 1990;94:5154.
- [34] Peng ZA, Peng XG. *J Am Chem Soc* 2001;123:1389.